# NMR Investigation and Dynamic Behaviour of [2,2′-Bipyridylbis(pyridine)platinum(II)]$^{2+}$ and Related Cationic Complexes − Crystal Structure of $[Pt(bipy)(py)_2](PF_6)_2$

**Enrico Rotondo,*[a] Giuseppe Bruschetta,[a] Giuseppe Bruno,[a] Archimede Rotondo,[a] Maria Letizia Di Pietro,[a] and Matteo Cusumano[a]**

**Keywords:** Intercalations / N ligands / NMR spectroscopy / Platinum

Detailed $^1$H and $^{13}$C{$^1$H} NMR analysis has been carried out on complexes with the general formulae $[Pt(bipy)(n\text{-}Rpy)_2](PF_6)_2$ and $[Pt(4\text{-}Phbipy)(n\text{-}Rpy)_2](PF_6)_2$ [bipy = 2,2′-bipyridyl; 4-Phbipy = 4,4′-diphenyl-2,2′-dipyridyl; *n*-Rpy = pyridine or substituted pyridines]. The resonance assignments and X-ray structures of these complexes are important steps on our route to: (i) interpretation of the intercalative geometry on the basis of the magnetic changes produced on interaction with DNA, (ii) rational design of new intercalators. The X-ray structure of the parent complex $[Pt(bipy)(py)_2](PF_6)_2$ (py = pyridine) shows pyridine rings quasiperpendicular to the coordination plane. In solution, because of the hindered rotation about Pt–N bonds of *ortho*- and *meta*-monosubstituted pyridines, this arrangement leads to "head-to-head" *s-cis* $C_s$ and "head-to-tail" *s-trans* $C_2$ rotamers in equilibrium. NMR line shape and $^{13}$C relaxation time constant measurements were carried out in order to evaluate activation energies and anisotropic rotational motion of *n*-Rpy. In some of these complexes a second dynamic process could be frozen on the $^{13}$C NMR timescale below 265 K. This lower activation energy process can reasonably be attributed to minimal bipyridyl torsion angle flipping driving a concerted molecular motion about the core of the four N-donors. Indeed, the X-ray structure of **1** proves distortion with a slight alternate up and down shift of the four nitrogen atoms about the coordination plane. Significantly, the fast rotation of unhindered pyridine rings does not allow NMR detection of this molecular distortion.


## Introduction

Energy barriers for rotation about Pt−N bonds and the fluxional behaviour of rotational isomers of $Pt^{II}$ square-planar complexes have attracted renewed interest in the last decade. These barriers are, in fact, important factors in stereocontrolled transition metal mediated self-assembly.[1] On the other hand, Pt−N(guanine) (or -adenine) rotational barriers can play key roles in inhibition of DNA duplication ensuing $Pt^{II}$−purine base inter- and intra-strand bond formation.[2] In the course of studies concerning the interactions of square-planar complexes and DNA[3] we have reported the intercalating properties of **7**.[4] Our attention was then attracted by complexes of general formulae $[Pt(bipy)(n\text{-}Rpy)_2](PF_6)_2$ and $[Pt(4\text{-}Phbipy)(n\text{-}Rpy)_2](PF_6)_2$ (**1**−**9**, Scheme 1).

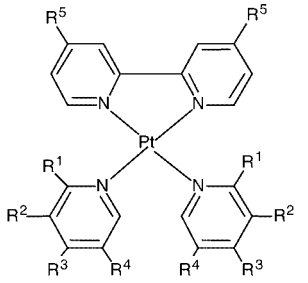

| | 1 | 2 | 3 | 4 | 5 | 6 | 7 | 8 | 9 |
|---|---|---|---|---|---|---|---|---|---|
| $R^1$ | H | $CH_3$ | H | H | H | H | H | H | H |
| $R^2$ | H | H | $CH_3CN$ | Ph | H | $CH_3$ | H | H | |
| $R^3$ | H | H | H | H | H | Ph | H | H | CN |
| $R^4$ | H | H | H | H | H | H | $CH_3$ | H | |
| $R^5$ | H | H | H | H | H | H | H | Ph | Ph |

Scheme 1

Indeed, the flat Pt(bipy) moiety is particularly well suited to intercalate DNA, whereas the rotational barriers of coordinated *n*-Rpy and phenyl substituents might either prevent or allow more extended intercalation, depending on the energy necessary to induce other aromatic rings to lay in the coordination plane.

Despite the popularity of such $[Pt(bipy)(n\text{-}Rpy)_2](PF_6)_2$ complexes, there are only a few NMR spectroscopic data concerning them. The aim of this paper is to provide NMR resonance assignments, together with dynamic and struc-

[a] Dipartimento di Chimica Inorganica, Analitica, e Chimica Fisica, Facotà di Scienze, Università di Messina,
Salita Sperone 31, 98166 Messina, Italia
E-mail: rotondo@chem.unime.it

  **DOI: 10.1002/ejic.200300032** 

tural features of these molecules, in particular highlighting pyridine rotation about the Pt−N bond. These properties are fundamental for mapping of the complexes' intercalative geometries and for rational design of new intercalator families.

## Results and Discussion

### NMR Analysis

Tables 1 and 2 report selected $^1$H and $^{13}$C{$^1$H} NMR resonance frequencies of **1**−**9**. Peak assignments are supported by conventional 1D and 2D homo- and heteronuclear experiments. Unambiguous resonance assignments, as well as structural feature determinations, are obligatory steps in any NMR attempt to shed light on the DNA double helix intercalative geometries of these complexes.[5] All reported crystal structures of [Pt(bipy)(*n*-Rpy)$_2$]$^{2+}$ cations concordely showed orientations of the heteroaromatic pyridine rings quasiperpendicular to the coordination plane.[4,6] The X-ray structure of [Pt(bipy)(*n*-Rpy)$_2$](PF$_6$)$_2$ shown here confirms this arrangement, which forces the 6,6′-bipy protons to point toward the centre of the pyridine's ring current. NMR spectra consistently show a shift of the 6,6′-H(bipy) signals by about 1 ppm to lower frequency with respect to the analogous [Pt(bipy)(am)$_2$](PF$_6$)$_2$ (am = mono- and bidentate aliphatic amines) resonances.[7] The anisotropic diamagnetic shifts of 6,6′-bipy proton signals, monitored both for substituted and for unsubstituted pyridines, suggest that, in solution, the heteroaromatic rings preserve the quasiperpendicular orientation shown in the crystal structure. This preferred orientation does not, however, rule out the possibility of rotation. In order to obtain more clues relating to the capabilities of the aromatic rings in these molecules to rotate about the Pt−N bond, we measured and compared spin lattice relaxation time constants of selected $^{13}$C atoms in **1**, **2**, **5** and **8**. Under decoupling conditions and for purely dipolar relaxations of aromatic C−H in the extreme narrowing limit, the Equation below applies.[8]

$$1/T_{1-DD} = \rho_{C\text{-}DD} = \tau_C [\gamma_H^2\gamma_C^2\eta^2/r^6]$$

If contributions of not directly attached protons are neglected and the C−H distance considered constant, relaxation time constants can be taken as a measure of the aromatic ring anisotropic spin diffusion. For aromatic ring carbon atoms bonded to fragments sufficiently large to be regarded as fixed matrices, diffusion preferentially occurs by rotation about the connection axis. This relatively fast motion slows down the relaxation rates of *ortho*- and *meta*-carbon atoms without altering the *para*-carbon atoms, the proton-attached dependent local fields of which are not affected by the rotation.[8,9] On this basis, the time constants ($T_1$) at room temperature are consistent with rotation of pyridine, *para*-substituted pyridine and phenyl rings, and hindered rotation of *meta*- and *ortho*-substituted pyridine rings (Table 3).

Table 1. $^1$H NMR chemical shifts [ppm] of **1**−**9** in [D$_6$]acetone at 298 K

| | bipy fragment | | | | Pyridine fragment | | | | | |
|---|---|---|---|---|---|---|---|---|---|---|
| | 3 | 4 | 5 | 6 | 2 | 3 | 4 | 5 | 6 | Me |
| **1** | 8.78 | 8.59 | 7.81 | 8.01 | 9.34 | 7.89 | 8.30 | 7.89 | 9.34 | |
| *trans*-**2** | 8.80 | 8.60 | 7.83 | 7.95 | | 7.91 | 8.19 | 7.63 | 9.21 | 3.34 |
| *cis*-**2** | 8.80 | 8.60 | 7.83 | 7.95 | | 7.91 | 8.19 | 7.70 | 9.46 | 3.49 |
| **3**[a] | 8.68 | 8.58 | 7.74 | 7.96 | 9.22 | | 8.11 | 7.72 | 9.12 | 2.45 |
| *trans*-**4** | 8.79 | 8.60 | 7.79 | 8.09 | 9.96 | | 8.73 | 8.13 | 9.68 | |
| *cis*-**4** | 8.79 | 8.60 | 7.79 | 8.09 | 9.92 | | 8.73 | 8.13 | 9.73 | |
| *trans*-**5** | 8.79 | 8.59 | 7.81 | 8.17 | 9.77 | | 8.56 | 7.96 | 9.41 | |
| *cis*-**5** | 8.79 | 8.59 | 7.81 | 8.17 | 9.75 | | 8.56 | 7.93 | 9.37 | |
| **6** | 8.78 | 8.58 | 7.82 | 8.12 | 9.37 | 8.19 | | 8.19 | 9.37 | |
| **7** | 8.84 | 8.64 | 7.81 | 7.96 | 9.08 | | 7.96 | | 9.08 | 2.38 |
| **8** | 9.29 | | 8.09 | 8.03 | 9.39 | 7.91 | 8.33 | 7.91 | 9.39 | |
| **9** | 9.32 | | 8.07 | 8.07 | 9.78 | 8.38 | | 8.38 | 9.78 | |

[a] *cis* and *trans* rotamer resonances overlapped within 0.01 ppm throughout.

Table 2. Selected $^{13}$C{$^1$H} NMR chemical shifts [ppm] of **1**−**9** in [D$_6$]acetone at 298 K

| | bipy fragment | | | | | Pyridine fragment | | | | |
|---|---|---|---|---|---|---|---|---|---|---|
| | 2 | 3 | 4 | 5 | 6 | 2 | 3 | 4 | 5 | 6 |
| **1** | 157.6 | 125.6 | 143.7 | 129.7 | 151.0 | 153.4 | 129.6 | 142.9 | 129.6 | 153.4 |
| *trans*-**2** | 161.9 | 125.6 | 143.8 | 129.9 | 150.6 | 158.0 | 130.1 | 142.2 | 126.2 | 153.8 |
| *cis*-**2** | 161.9 | 125.6 | 143.8 | 129.9 | 150.8 | 157.9 | 130.3 | 142.3 | 126.2 | 152.7 |
| *trans*-**3**[a] | 157.6 | 125.7 | 143.8 | 129.7 | 151.1 | 153.2 | 140.5 | 143.4 | 128.8 | 150.6 |
| *cis*-**3**[a] | 157.6 | 125.7 | 143.8 | 129.7 | 151.1 | 153.0 | 140.5 | 143.4 | 128.8 | 150.5 |
| *trans*-**4**[a] | 157.2 | 125.5 | 143.9 | 129.5 | 151.4 | 156.9 | 114.7 | 145.8 | 130.0 | 156.6 |
| cis-**4**[a] | 157.2 | 125.5 | 143.9 | 129.5 | 151.4 | 156.7 | 114.7 | 145.8 | 129.9 | 156.3 |
| *trans*-**5**[a] | 157.5 | 125.7 | 143.8 | 129.7 | 151.3 | 151.1 | 142.1 | 140.5 | 129.5 | 151.8 |
| *cis*-**5**[a] | 157.5 | 125.7 | 143.8 | 129.7 | 151.3 | 151.3 | 142.0 | 140.5 | 129.5 | 151.7 |
| **6** | 157.6 | 125.7 | 143.8 | 129.7 | 151.1 | 153.3 | 126.4 | 153.6 | 126.4 | 153.3 |
| **7** | 157.4 | 125.6 | 143.6 | 129.7 | 151.1 | 150.2 | 139.5 | 143.9 | 139.5 | 150.2 |
| **8** | 158.0 | 123.4 | 154.9 | 126.4 | 151.1 | 153.6 | 129.7 | 143.0 | 129.7 | 153.6 |
| **9** | 157.8 | 123.6 | 155.2 | 126.3 | 151.3 | 155.0 | 131.9 | 126.0 | 131.9 | 155.0 |

[a] Assignments for the two rotamers could be inverted.

Table 3. $^{13}$C relaxation time constants [s] of selected aromatic C−H carbon atoms in [D$_6$]acetone at 298 K; standard deviations are less than 5%

| | bipy | | | | Pyridine | | | Phenyl | | |
|---|---|---|---|---|---|---|---|---|---|---|
| | C-3 | C-4 | C-5 | C-6 | C-*ortho* | C-*meta* | C-*para* | C-*ortho* | C-*meta* | C-*para* |
| **1** | 1.4 | 1.4 | 1.4 | 1.5 | 1.9 | 1.8 | 1.3 | | | |
| **2**[a] | 1.3 | 1.2 | 1.1 | 1.3 | 1.2 | 1.1 | 1.2 | | | |
| **5**[a] | 1.1 | nd | 0.9 | 1.0 | 1.4 | 1.3 | 1.2 | 1.9 | 1.7 | 1.2 |
| **8** | 0.9 | | 1.0 | 1.1 | 1.7 | 1.7 | 1.0 | 1.8 | 1.8 | 1.1 |

[a] No appreciable time constant differences found for the two rotamers.

For *ortho*- and *meta*-monosubstituted bis(pyridine) complexes the quasiperpendicular orientation implies the existence of "head-to-tail" *s-trans* and "head-to-head" *s-cis* rotamers of $C_2$ and $C_s$ symmetry, respectively (two enantiomers can be envisaged for the $C_2$ molecules, owing to the chirality axes). The rates of these stereoisomer interconvertions depend on the lower activation energy path either

  

of a dissociative step involving Pt−N bond breaking, or of a single pyridine asynchronous rotation about the Pt−N bond. The NMR spectra of the monosubstituted pyridine complexes at 298 K show the resonances of the two rotamers in slow exchange on the NMR timescale. Signal integration showed approximately equal thermodynamic stability between rotamer couples. Resonance assignments (which rotamer is which) were made, when feasible, through positive NOEs between methyl (or aryl) groups and the opposite proton of the adjacent *cis*-pyridine (6-H for 2- and 5-H for 3-monosubstituted pyridines, respectively) observed for the $C_s$ but not for the $C_2$ configurations (Scheme 2).

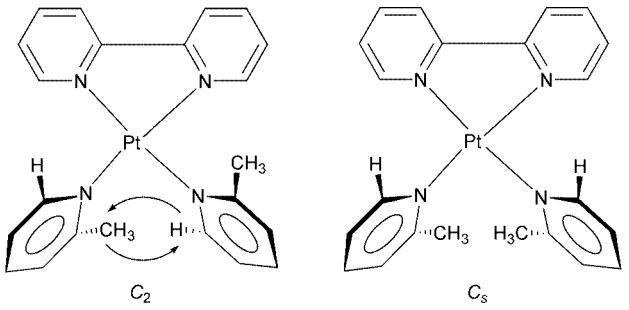


Scheme 2. Two-dimensional representation, symmetry and NOE contacts of the two rotamers of **2**

Pyridine-nitrogen, *ortho*-carbon and -proton resonances were used as probes for the conformational line shape analysis. The activation energy for rotamer interchange, calculated at coalescence, strongly differs as a function of the substituent position. We could not detect coalescence for 2-Mepy rotamers **2** even at 430 K in [$D_6$]DMSO ($\Delta G^{\neq} >$ 130 kJ), while 3-substituted pyridines **3**, **4** and **5**, in acetone, showed an activation energy of about 70 kJ (Table 4). The difference can be attributed to steric interactions between ligands differently hindering the pyridine crossing of coordination planes. The displacement of solvent molecules required by rotation, electronic effect of substituents on the Pt−N bond and, perhaps, stacking interactions between *cis*-pyridines may make contributions to these activation energies. These results are not consistent with a dissociative mechanism, which can also be ruled out on the basis of the permanence, above the coalescence temperatures, of $^{195}$Pt satellites in the 2/6-py $^1$H resonances.

Table 4. Activation energies for asynchronous rotation about the Pt−N bonds of monosubstituted bis(pyridine) complexes ($\Delta G^{\neq}_{(1)}$) and for molecular concerted distortion ($\Delta G^{\neq}_{(2)}$)

| | $\Delta G^{\neq}_{(1)}$ [kJ·mol$^{-1}$] | $\Delta G^{\neq}_{(2)}$ [kJ·mol$^{-1}$] |
|---|---|---|
| **2** (2-Me-py) | > 130 | 57 ± 2 (265 K) |
| **4** (3-CN-py) | 71.9 ± 1 (326 K) | 57 ± 2 (265 K) |
| **5** (3-Ph-py) | 71.6 ± 1 (323 K) | 57 ± 2 (265 K) |
| **3** (3-Me-py) | 68.5 ± 1 (320 K) | 57 ± 2 (265 K) |

At 240 K, the $^{13}$C{$^1$H} NMR spectrum of **3** showed the doubling of the C-2 and C-6 resonances as a consequence of a second dynamic process (Figure 1). At the same temperature, analogous carbon resonance splitting was observed for the other *ortho*- and *meta*-monosubstituted pyridine complexes. We suggest these splittings are due to freezing of square-planar-distorted conformations. As a matter of fact, the solid-state structure of **1** shows a small, propeller-like torsion of the bipyridyl rings about the C2−C2′ axis, displacing the N donors slightly out of the coordination plane. The X-ray structure also shows a "bumping" of bipy, constraining the pyridine's N3−Pt−N4 angle (about 80°). The 6,6′-H of slightly distorted bipy pushes the two opposite pyridines up and down the ring centre, respectively, causing a distortion of the ring planes by about 10° with respect to the perpendicular alignment. Steric crowding also forces the nitrogen donors of the Pt−N4 core alternatively up and down the mean coordination plane. Concerted bipy torsion angle flipping, pyridine ring windscreen-wiper rocking and up and down N-donors twisting about the mean coordination plane create a time-averaged planar symmetry for the bis(pyridine) complex. At low temperatures, freezing of the concerted flipping destroys the bipy averaged planarity, doubling the number of *ortho*- and *meta*-monosubstituted *s-trans* conformers. Indeed, the "frozen" $C_2$ propeller-like torsion of bipy generates two pairs of diastereomers from the two monosubstituted *s-trans* Δ and Λ enantiorotamers: namely ΔΔ′ and ΔΛ′ arising from the original Δ rotamer, and the corresponding enantiomers ΛΔ′ and ΛΛ′ from the original Λ rotamer (Scheme 3). On the other side, the *s-cis* rotamer is split into an enantiomer couple of $C_1$ symmetry, whose *cis*-pyridine nuclei resonate, in principle, at different frequencies. Significantly, only the C-2 and the C-6 pyridine nuclei, because of their preferential observation positions just on the top of the bipy moiety, double their resonances, indicating the molecular distortion freezing at low temperature.

In conclusion, variable-temperature spectra of rotamers show two different fluxional processes. We attribute the lower activation energy barrier to overall concerted flipping. The higher barrier must be due to asynchronous rotation of a single pyridine moiety about the Pt−N bond. In principle, simultaneous 180° rotation of the two heteroaromatic rings can physically not be distinguished from bipy flipping driving the concerted molecular motion. It is known, however,[10] that simultaneous rotation of both pyridines has a larger activation energy than the asynchronous single-ring rotation, so it seems reasonable to attribute the low fluxional activation energy to concerted flipping and the higher to the asynchronous rotation. No splitting of the resonances at low temperatures was observed for pyridine and *para*-substituted pyridine complexes **1**, **6**, **8** and **9**. This is consistent with low rotational barriers of these unhindered pyridines, which do not allow detection, at low temperatures, of bipy torsion freezing.

### Discussion of Structure 1

Although **1** is the parent complex of an interesting class of metal species, the crystal structure, reported here with the $PF_6^-$ counter ion, was not previously available. The

  

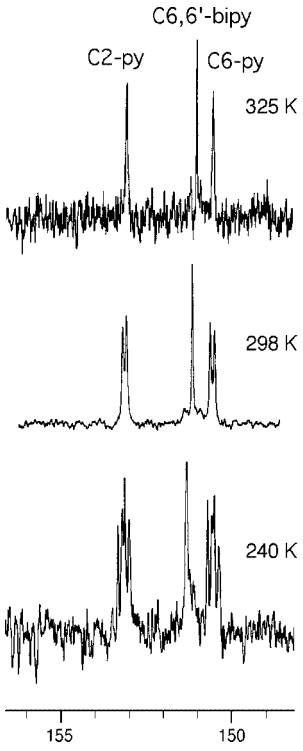


Figure 1. $^{13}C\{^1H\}$ spectra of **3** run at different temperatures

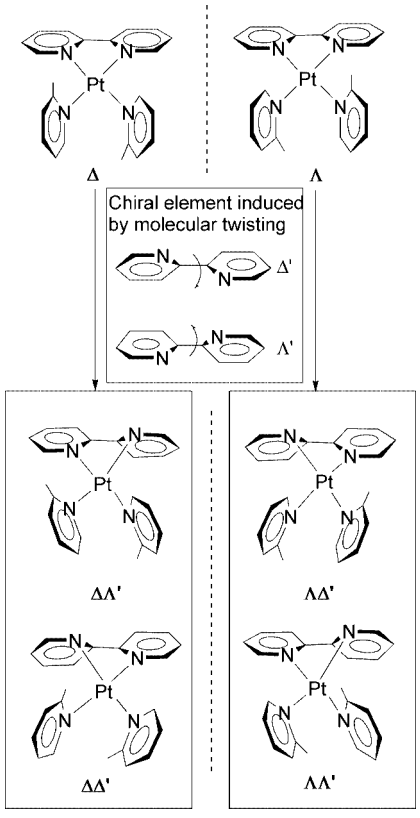


Scheme 3. Splitting due to the freezing of the $C_2$ twisting

complex crystallizes in the $P\bar{1}$ space group with one molecule in the asymmetric unit. The expected square-planar geometry is evident for the Pt coordination, whereas the anions show the usual octahedral conformation with just slight distortions (Figure 2 and Tables 5−7).

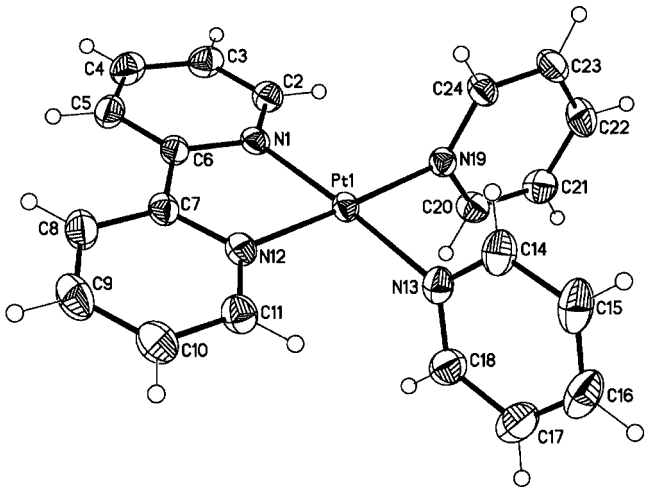


Figure 2. ORTEP view for the positively charged part of **1** with thermal ellipsoids to 30% of probability

Table 5. Crystal data and structure refinement for **1**

| | |
|---|---|
| Empirical formula | $C_{20}H_{18}F_{12}N_4P_2Pt$ |
| Formula mass | 799.41 |
| Temperature | 298(2) K |
| Wavelength | 0.71073 Å |
| Crystal system | triclinic |
| Space group | $P\bar{1}$ |
| Unit cell dimensions | $a$ = 8.5573(13) Å; α = 79.661(12)° |
| | $b$ = 10.9811(19) Å; β = 77.035(12)° |
| | $c$ = 14.671(2) Å; γ = 71.971(12)° |
| Volume | 1268.4(4) Å$^3$ |
| $Z$ | 2 |
| Density (calcd.) | 2.093 Mg/m$^3$ |
| Absorption coefficient | 5.764 mm$^{-1}$ |
| $F$(000) | 764 |
| Crystal size | 0.58 × 0.46 × 0.32 mm |
| Θ range for data collection | 1.96−27.50° |
| Index ranges | $-10 \le h \le 1$, $-14 \le k \le 13$, |
| | $-19 \le l \le 18$ |
| Reflections collected | 6822 |
| Independent reflections | 5657 [$R$(int) = 0.0214] |
| Completeness to Θ = 27.50° | 97.1% |
| Absorption correction | empirical |
| Max. and min. transmission | 0.2458 and 0.0801 |
| Refinement method | full-matrix least-squares on $F^2$ |
| Data/restraints/parameters | 5657/72/353 |
| Goodness-of-fit on $F^2$ | 1.068 |
| Final $R$ indices [$I > 2\sigma(I)$] | $R_1$ = 0.0255, $wR_2$ = 0.0605 |
| $R$ indices (all data) | $R_1$ = 0.0325, $wR_2$ = 0.0646 |
| Extinction coefficient | 0.0112(5) |
| Largest diff. peak and hole | 1.558 and −1.396 e·Å$^{-3}$ |

This square coordination plane is almost planar [max. deviation from the mean plane: N13 −0.0585(2) Å], though the bipyridyl short-bite strains the coordination angles and although the molecular symmetry is $C_{2v}$, the platinum atom is not able to occupy a special crystallographic position. The Pt−N distances are consistent with previously reported analogous crystal structures (Table 6).[3b,11,12]

  

Table 6. Selected bond lengths [Å] and angles [°] for **1**

| | | | |
|---|---|---|---|
| Pt1−N1 | 2.002(3) | Pt1−N12 | 2.002(3) |
| Pt1−N13 | 2.019(3) | Pt1−N19 | 2.024(3) |
| N1−C6 | 1.361(5) | C6−C7 | 1.467(6) |
| C7−N12 | 1.356(5) | C11−N12 | 1.338(5) |
| N1−Pt1−N12 | 81.01(13) | N1−Pt1−N13 | 176.38(13) |
| N12−Pt1−N13 | 96.85(14) | N1−Pt1−N19 | 97.69(13) |
| N12−Pt1−N19 | 177.27(12) | N13−Pt1−N19 | 84.57(13) |
| C2−N1−Pt1 | 125.7(3) | C6−N1−Pt1 | 114.7(3) |
| C7−C8−C9 | 119.5(5) | C10−C9−C8 | 119.1(4) |
| C11−N12−Pt1 | 126.1(3) | C7−N12−Pt1 | 114.9(3) |

Table 7. Hydrogen bonds for **1** [Å and °]; symmetry transformations used to generate equivalent atoms: #1: $-x+1, -y+1, -z+2$; #2: $-x+1, -y+2, -z+1$; #3: $-x+2, -y+1, -z+1$

| D−H···A | *d*(D−H) | *d*(H···A) | *d*(D···A) | <(DHA) |
|---|---|---|---|---|
| C(11)H(11)···F(2)#1 | 0.93 | 2.49 | 3.237(6) | 137.4 |
| C(23)H(23)···F(11)#2 | 0.93 | 2.51 | 3.390(6) | 157.1 |
| C(3)H(3)···F(7)#3 | 0.93 | 2.51 | 3.261(6) | 138.4 |

The bipy plane almost overlaps the coordination plane [angle between mean planes: 3.69(8)°], while, as already observed in the cited papers,[3b,11,12] the pyridine aromatic rings are almost perpendicular to the coordination plane [angles between mean planes: 80.2(2)° and 80.8(1)°].

These moieties are not pointing directly toward the metal atom, which is slightly out from the pyridine averaged planes [0.196(1) and −0.323(1) Å]. This "clamp-like" closure may reasonably be due to the steric bumping of the pyridines against the bipy "wings", which is also consistent with the slightly greater corresponding strain detected for the palladium analogues.[13]

Other than the usual intermolecular hydrogen bonds, in which three fluorine atoms play the acceptor roles (see Tables), remarkable dipolar interactions take place between the fluorine and the metal atoms along the apical positions

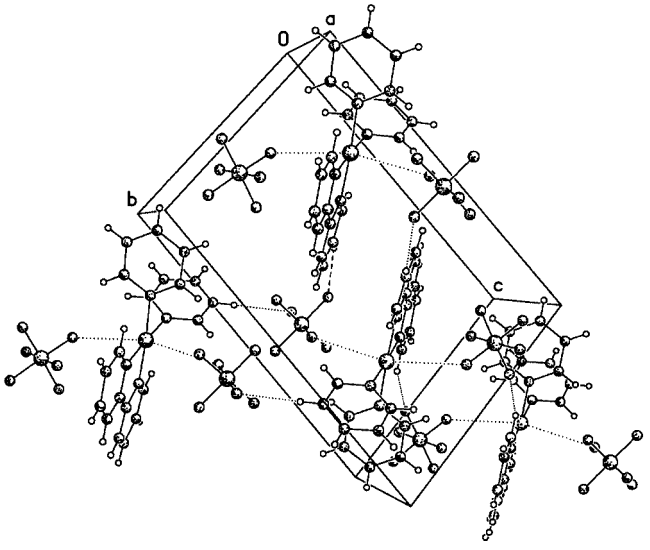


Figure 3. ORTEP view of the cell crystal packing for **1**

[Pt1···F5 3.298(5), Pt1···F8 3.338(5) Å]. These distances are shorter than those measured when pyridine is branched, probably because of steric hindrance.[3] Moreover, an intermolecular stacking interaction is present between the same ring of two bipyridyl moieties related by a symmetry inversion centre [distance between the two perfectly parallel planes: 3.339(1) Å].

All these attracting interactions produce three different types of dimeric aggregates in which the two units are related by an inversion centre and at least two pairs of interactions (see Figure 3).

## Experimental Section

**General:** $^1$H and $^{13}C\{^1H\}$ NMR spectra were recorded with a Bruker ARX 300 spectrometer, at 300.13 and 75.47 MHz, respectively. The $^1$H NMR spectra were calibrated against the residual proton signals of the solvent as internal reference ([D$_6$]acetone: δ = 2.04 ppm), the $^{13}C\{^1H\}$ spectra were calibrated against the septuplet of the solvent ([D$_6$]acetone: δ = 29.80 ppm); $^{13}C\{^1H\}$ spin-lattice relaxation time constants were measured under $N_2$ by the "inversion recovery"[14] sequence.

**Synthesis:** The complexes were prepared by a previously described general procedure,[3,4] by heating of an aqueous suspension of [Pt(bipy)Cl$_2$] with an excess of the appropriate pyridine derivative at reflux. After dissolution of the solid, $NH_4PF_6$ was added and the resulting complexes [Pt(bipy)(*n*-Rpy)$_2$](PF$_6$)$_2$ precipitated as white or pale yellow substances, which were recrystallized from water/acetone. Elemental analyses were performed at the Microanalytical Laboratory of Redox snc (Milano).

**[Pt(bipy)(py)$_2$](PF$_6$)$_2$ (1):** $^1$H NMR (300 MHz, [D$_6$]acetone): δ = 9.34 (dd, $^3J$ = 5.1, $^4J$ = 1.5 Hz, 4 H, 2-py, 6-py), 8.78 (d, $^3J$ = 8.2 Hz, 2 H, 3,3′-bipy), 8.59 (td, $^3J$ = 7.9, $^4J$ = 1.4 Hz, 2 H, 4,4′-bipy), 8.30 (tt, $^3J$ = 7.7, $^4J$ = 1.5 Hz, 2 H, 4-py), 8.01 (m, 2 H, 6,6′-bipy), 7.89 (m, 4 H, 3-py, 5-py), 7.81 (m, 2 H, 5,5′-bipy) ppm. $^{13}C\{^1H\}$ NMR (75 MHz, [D$_6$]acetone): δ = 157.6 (2 C, 2,2′-bipy), 153.4 (4 CH, 2-py, 6-py), 151.0 (2 CH, 6,6′-bipy), 143.7 (2 CH, 4,4′-bipy), 142.9 (2 CH, 4-py), 129.7 (2 CH, 5,5′-bipy), 129.6 (4 CH, 3-py, 5-py), 125.6 (2 CH, 3,3′-bipy) ppm. $C_{20}H_{18}F_{12}N_4P_2Pt$ (799): calcd. C 30.03, H 2.25, N 7.01; found C 30.11, H 2.38, N 7.09.

**(*s-cis*/*s-trans*)-[Pt(bipy)(2-Mepy)$_2$](PF$_6$)$_2$ (2):** $^1$H NMR (300 MHz, [D$_6$]acetone): δ = 9.46, 9.21 (dd, $^3$ = 5.6, $^4J$ = 1.5 Hz, 2 H/2 H, 6-py), 8.80 (d, $^3J$ = 7.7 Hz, 4 H, 3,3′-bipy), 8.60 (td, $^3J$ = 7.9, $^4J$ = 1.4 Hz, 4 H, 4,4′-bipy), 8.19 (m, 4 H, 4-py), 7.95 (m, 4 H, 6,6′-bipy), 7.91 (m, 4 H, 3-py), 7.83 (m, 4 H, 5,5′-bipy), 7.70, 7.63 (td, $^3J$ = 7.7, $^4J$ = 1.4 Hz, 2 H/2 H, 5-py), 3.49, 3.34 (s, 6 H/6 H, CH$_3$) ppm. $^{13}C\{^1H\}$ NMR (75 MHz, [D$_6$]acetone): δ = 161.9 (4 C, 2,2′-bipy), 158.0, 157.9 (2 C/2 C, 2-py), 153.8, 152.7 (2 CH/2 CH, 6-py), 150.8, 150.6 (2 CH/2 CH, 6,6′-bipy), 143.8 (4 CH, 4,4′-bipy), 142.2, 142.3 (2 CH/2 CH, 4-py), 130.3, 130.1 (2 CH/2 CH, 3-py), 129.9 (4 CH, 5,5′-bipy), 126.2 (4 CH, 5-py), 125.6 (4 CH, 3,3′-bipy), 27.1, 26.5 (2 CH$_3$/2 CH$_3$) ppm. $C_{22}H_{22}F_{12}N_4P_2Pt$ (827): calcd. C 31.92, H 2.66, N 6.77; found C 32.20, H 2.78, N 6.88.

**(*s-cis*/*s-trans*)-[Pt(bipy)(3-Mepy)$_2$](PF$_6$)$_2$ (3):** $^1$H NMR (300 MHz, [D$_6$]acetone): δ = 9.22 (s, 4 H, 2-py), 9.12 (s, 4 H, 6-py), 8.68 (d, $^3J$ = 7.7 Hz, 4 H, 3,3′-bipy), 8.58 (td, $^3J$ = 7.7, $^4J$ = 1.4 Hz, 4 H, 4,4′-bipy), 8.11 (d, $^3J$ = 7.6 Hz, 4 H, 4-py), 7.96 (d, $^3J$ = 5.6 Hz, 4 H, 6,6′-bipy), 7.74 (m, 4 H, 5,5′-bipy), 7.72 (m, 4 H, 5-py), 2.45

  

(s, 12 H, $CH_3$) ppm. $^{13}C\{^1H\}$ NMR (75 MHz, [$D_6$]acetone): δ = 157.6 (4 C, 2,2′-bipy), 153.2, 153.0 (2 CH:2 CH, 2-py), 151.1 (4 CH, 6,6′-bipy), 150.6, 150.5 (2 CH:2 CH, 6-py), 143.8 (4 CH, 4,4′-bipy), 143.4 (4 CH, 4-py), 140.5 (4 C, 3-py), 129.7 (4 CH, 5,5′-bipy), 128.8 (4 CH, 5-py), 125.7 (4 CH, 3,3′-bipy), 18.4 (4 $CH_3$) ppm. $C_{22}H_{22}F_{12}N_4P_2Pt$ (827): calcd. C 31.92, H 2.66, N 6.77; found C 32.17, H 2.76, N 6.88.

**(*s-cis*/*s-trans*)-[Pt(bipy)(3-CNpy)$_2$](PF$_6$)$_2$ (4):** $^1H$ NMR (300 MHz, [$D_6$]acetone): δ = 9.96, 9.92 (s, 2 H:2 H, 2-py), 9.73, 9.68 (d, $^3J$ = 7.8 Hz, 2 H:2 H, 6-py), 8.79 (d, $^3J$ = 7.9 Hz, 4 H, 3,3′-bipy), 8.73 (m, 4 H, 4-py), 8.60 (td, $^3J$ = 7.9, $^4J$ = 1.4 Hz, 4 H, 4,4′-bipy), 8.13 (m, 4 H, 5-py), 8.09 (m, 4 H, 6,6′-bipy), 7.79 (td, $^3J$ = 7.9, $^4J$ = 1.5 Hz, 4 H, 5,5′-bipy) ppm. $^{13}C\{^1H\}$ NMR (75 MHz, [$D_6$]acetone): δ = 157.2, (4 C, 2,2′-bipy), 156.9, 156.7 (2 CH:2 CH, 2-py), 156.6, 156.3 (2 CH:2 CH, 6-py), 151.4 (4 CH, 6,6′-bipy), 145.8 (4 CH, 4-py), 143.9 (4 CH, 4,4′-bipy), 130.0, 129.9 (4 CH, 5-py), 129.5 (4 CH, 5,5′-bipy), 125.5 (4 CH, 3,3′-bipy), 115.5 (4 CN), 114.7 (4 C, 3-py) ppm. $C_{22}H_{16}F_{12}N_6P_2Pt$ (849): calcd. C 31.09, H 1.88, N 9.89; found C 30.65, H 2.01, N 10.01.

**(*s-cis*/*s-trans*)-[Pt(bipy)(3-Phpy)$_2$](PF$_6$)$_2$ (5):** $^1H$ NMR (300 MHz, [$D_6$]acetone): δ = 9.77, 9.75 (s, 2 H:2 H, 2-py), 9.41, 9.37 (dd, $^3J$ = 5.6, $^4J$ = 1.5 Hz, 2 H:2 H, 6-py), 8.79 (d, $^3J$ = 7.7 Hz, 4 H, 3,3′-bipy), 8.59 (m, 4 H, 4,4′-bipy), 8.56 (m, 4 H, 4-py), 8.17 (m, 4 H, 6,6′-bipy), 7.96, 7.93 (td, $^3J$ = 7.7, $^5J$ = 1.3 Hz, 2 H:2 H, 5-py), 7.81 (m, 4 H, 5,5′-bipy), 7.75 (m, 8 H, *o*-Ph), 7.54 (m, 8 H, *m*-Ph), 7.47 (m, 4 H, *p*-Ph) ppm. $^{13}C\{^1H\}$ NMR (75 MHz, [$D_6$]acetone): δ = 157.5 (4 C, 2,2′-bipy), 151.8, 151.7 (2 CH/2 CH, 6-py), 151.3 (4 CH, 6,6′-bipy), 151.3, 151.1 (2 CH/2 CH, 2-py), 143.8 (4 CH, 4,4′-bipy), 142.1, 142.0 (2 C/2 C, 3-py), 140.5 (4 CH, 4-py), 135.2 (4 C, $C_{ipso}$), 130.6, 130.5 (2 CH/2 CH, *p*-Ph), 130.2 (8 CH, *m*-Ph), 129.7 (4 CH, 5,5′-bipy), 129.5 (4 CH, 5-py), 128.2 (8 CH, *o*-Ph), 125.7 (4 CH, 3,3′-bipy) ppm. $C_{32}H_{26}F_{12}N_4P_2Pt$ (951): calcd. C 40.37, H 2.73, N 5.89; found C 40.11, H 2.98, N 6.05.

**[Pt(bipy)(4-Phpy)$_2$](PF$_6$)$_2$ (6):** $^1H$ NMR (300 MHz, [$D_6$]acetone): δ = 9.37 (dd, $^3J$ = 5.1, $^5J$ = 1.3 Hz, 4 H, 2-py, 6-py), 8.78 (d, $^3J$ = 8.2 Hz, 2 H, 3,3′-bipy), 8.58 (td, $^3J$ = 8.2, $^4J$ = 1.4 Hz, 2 H, 4,4′-bipy), 8.19 (dd, $^3J$ = 5.1, $^5J$ = 1.3 Hz, 4 H, 3-py, 5-py), 8.12 (m, 2 H, 6,6′-bipy), 7.93 (m, 4 H, *o*-Ph), 7.82 (td, $^3J$ = 7.9, $^4J$ = 1.4 Hz, 2 H, 5,5′-bipy), 7.58 (overlapped m, 6 H, *m*-Ph, *p*-Ph) ppm. $^{13}C\{^1H\}$ NMR (75 MHz, [$D_6$]acetone): δ = 157.6 (2 C, 2,2′-bipy), 153.6 (2 C, 4-py), 153.3 (4 CH, 2-py, 6-py), 151.1 (2 CH, 6,6′-bipy), 143.8 (2 CH, 4,4′-bipy), 135.5 (2 C, $C_{ipso}$), 132.1 (2 CH, *p*-Ph), 130.4 (4 CH, *m*-Ph), 129.7 (2 CH, 5,5′-bipy), 128.3 (4 CH, *o*-Ph), 126.4 (4 CH, 3-py, 5-py), 125.7 (2 CH, 3,3′-bipy) ppm. $C_{32}H_{26}F_{12}N_4PPt_2$ (951): calcd. C 40.37, H 2.73, N 5.89; found C 40.13, H 2.95, N 6.06.

**[Pt(bipy)(3,5-Me$_2$py)$_2$](PF$_6$)$_2$ (7):** $^1H$ NMR (300 MHz, [$D_6$]acetone): δ = 9.08 (s, 4 H, 2-py, 6-py), 8.84 (d, $^3J$ = 8.6 Hz, 2 H, 3,3′-bipy), 8.64 (td, $^3J$ = 8.6, $^4J$ = 1.5 Hz, 2 H, 4,4′-bipy), 7.96 (overlapped m, 4 H, 6,6′-bipy, 4-py), 7.82 (m, 2 H, 5,5′ bipy), 2.38 (s, 12 H, $CH_3$) ppm. $^{13}C\{^1H\}$ NMR (75 MHz, [$D_6$]acetone): δ = 157.4 (2 C, 2,2′-bipy), 151.1 (2 CH, 6,6′-bipy), 150.2 (4 CH, 2-py, 6-py), 143.9 (2 CH, 4-py), 143.6 (2 CH, 4,4′-bipy), 139.5 (4 C, 3-py, 5-py), 129.7 (2 CH, 5,5′-bipy), 125.6 (2 CH, 3,3′-bipy), 18.1 (4 $CH_3$) ppm. $C_{24}H_{26}F_{12}N_4P_2Pt$ (855): calcd. C 33.68, H 3.04, N 6.55; found C 33.07, H 2.91, N 6.87.

**[Pt(4-Phbipy)(py)$_2$](PF$_6$)$_2$ (8):** $^1H$ NMR (300 MHz, [$D_6$]acetone): δ = 9.39 (dd, $^3J$ = 5.1, $^4J$ = 1.5 Hz, 4 H, 2-py, 6-py), 9.29 (d, $^4J$ = 1.7 Hz, 2 H, 3,3′-bipy), 8.33 (tt, $^3J$ = 7.7, $^4J$ = 1.5 Hz, 2 H, 4-py), 8.09 (m, 2 H, 5,5′-bipy), 8.06 (m, 4 H, *o*-Ph), 8.03 (m, 2 H, 6,6′-bipy), 7.91 (m, 4 H, 3-py, 5-py), 7.65 (overlapped m, 6 H, *m*-Ph, *p*-Ph) ppm. $^{13}C\{^1H\}$ NMR (75 MHz, [$D_6$]acetone): δ = 158.0 (2 C, 2,2′-bipy), 154.9 (2 C, 4,4′-bipy), 153.6 (4 CH, 2-py, 6-py), 151.1 (2 CH, 6,6′-bipy), 143.0 (2 CH, 4-py), 135.7 (2 C, $C_{ipso}$), 132.4 (2 CH, *p*-Ph), 130.5 (4 CH, *m*-Ph), 129.7 (4 CH, 3-py, 5-py), 128.7 (4 CH, *o*-Ph), 126.4 (2 CH, 5,5′-bipy), 123.4 (2 CH, 3,3′-bipy) ppm. $C_{32}H_{26}F_{12}N_4P_2Pt$ (951): calcd. C 40.37, H 2.73, N 5.89; found C 40.16, H 2.99, N 6.04.

**[Pt(4-Phbipy)(4-CNpy)$_2$](PF$_6$)$_2$ (9):** $^1H$ NMR (300 MHz, [$D_6$]acetone): δ = 9.78 (dd, $^3J$ = 5.1, $^5J$ = 1.2 Hz, 4 H, 2-py, 6-py), 9.32 (d, $^4J$ = 1.7 Hz, 2 H, 3,3′-bipy), 8.38 (dd, $^3J$ = 5.1, $^5J$ = 1.2 Hz, 4 H, 3-py, 5-py), 8.07 (overlapped m, 8 H, 5,5′-bipy, 6,6′-bipy, *o*-Ph), 7.67 (overlapped m, 6 H, *m*-Ph, *p*-Ph) ppm. $^{13}C\{^1H\}$ NMR (75 MHz, [$D_6$]acetone): δ = 157.8 (2 C, 2,2′-bipy), 155.2 (2 C, 4,4′-bipy), 155.0 (4 CH, 2-py, 6-py), 151.3 (2 CH, 6,6′-bipy), 135.6 (2 C, $C_{ipso}$), 132.6 (2 CH, *p*-Ph), 131.9 (4 CH, 3-py, 5-py), 130.5 (4 CH, *m*-Ph), 128.7 (4 CH, *o*-Ph), 126.3 (2 CH, 5,5′-bipy), 126.0 (2 C, 4-py), 123.6 (2 CH, 3,3′-bipy), 115.5 (2 CN) ppm. $C_{34}H_{24}F_{12}N_6P_2Pt$ (1001): calcd. C 40.76, H 2.40, N 8.39; found C 40.60, H 2.45, N 8.41.

**Crystal Structure Determination of 1:** Crystals suitable for X-ray analysis were obtained by recrystallization from methanol solution. Diffraction data were collected from a colourless 0.58 × 0.46 × 0.32 mm irregular specimen at room temperature by use of a Siemens P4 automated four-circle single-crystal diffractometer with graphite-monochromated Mo-$K_\alpha$ radiation (λ = 0.71073 Å). Lattice parameters were obtained from least-squares refinement of the setting angles of 42 and 39 reflections within 5.34° ≤ θ ≤ 17.50° range. 6822 reflections were measured by the fixed speed θ-2θ scan technique up to 2θ ≤ 55°. No crystal decay was evidenced by reference reflections monitored each 197 measurements. Intensities were evaluated by profile fitting of a 96-step peak scan among 2θ shells procedure[15] and then corrected for Lorentz polarization effects. Absorption correction was applied by Gaussian integration of the indexed crystal shape. Data collection, reduction and face-indexed absorption correction were performed with the aid of the XSCANS[16] and SHELXTL packages.[17] The structure was solved by the Patterson standard method in the SHELXS package,[18] and refined by minimization of the function $\Sigma w(F_o^2 - F_c^2)^2$ by the full-matrix, least-squares technique based on all independent $F^2$, by use of SHELXL-97.[19] All non-hydrogen atoms were treated as anisotropic. Hydrogen atoms were placed in idealized positions and all the isotropic thermal parameters were fixed to the best fitting value. An empirical extinction parameter was included in the last refinement cycles. The last difference map showed expected electron density residuals close to the metal atoms (max. and min. values: 1.558 and −1.396 e·Å$^{-3}$). The final geometrical calculations and drawings were carried out with the aid of the PARST program[20] and the XPW[21] utility of the Siemens package, respectively. CCDC-201345 (**1**) contains the supplementary crystallographic data for this paper. These data can be obtained free of charge at www.ccdc.cam.ac.uk/conts/retrieving.html [or from the Cambridge Crystallographic Data Centre, 12 Union Road, Cambridge CB2 1EZ, UK; Fax: (internat.) + 44-1223/336-033; E-mail: deposit@ccdc.cam.ac.uk].

[1] R. Robson, B. F. Abrahams, S. R. Batten, R. W. Gable, B. F. Hoskins, J. Liu, *Supramolecular Architecture*, ACS Symposium Series 499 (Ed.: T. Bein), American Chemical Society, Washington D.C., **1992**, chapter 19. J.-C. Chambron, C. Dietrich-Buchecker, J.-P. Sauvage, "Transition Metals as Assembling and Templating Species", in: *Comprehensive Supramolecular Chemistry* (Ed.: J.-M. Lehn, Chair), Pergamon Press, Oxford, U.K., **1996**, vol. 9, chapter 2, p. 43.

  

[2] N. Margiotta, F. P. Fanizzi, J. Kobe, G. Natile, *Eur. J. Inorg. Chem.* **2001**, *5*, 1303−1310.
[3] [3a] M. Cusumano, A. Giannetto, *J. Inorg. Biochem.* **1997**, *65*, 137. [3b] M. Cusumano, M. L Di Pietro, A. Giannetto, *Inorg. Chem.* **1999**, *38*, 1754.
[4] M. Cusumano, M. L. Di Pietro, A. Giannetto, F. Nicolò, E. Rotondo, *Inorg. Chem.* **1998**, *37*, 563−568.
[5] C. M. Dupureur, J. K. Barton, *Inorg. Chem.* **1997**, *36*, 33−43; P. J. Dandliker, M. E. Núñez, J. K. Barton, *Biochemistry* **1998**, *37*, 6491−6502.
[6] F. H. Allen, J. E. Davies, J. J. Galloy, O. Johnson, O. Kennard, C. F. Macrae, E. M. Mitchell, G. F. Mitchell, J. M. Smith, D. G. Watson, *J. Chem. Info. Comp. Sci.* **1991**, *31*, 187.
[7] E. Rotondo, unpublished results.
[8] H.-O. Kalinowski, S. Berger, S. Braun, *Carbon-13 NMR Spectroscopy*, John Wiley & Sons, New York, **1988**.
[9] G. C. Levy, *J. Chem. Soc., Chem. Commun.* **1972**, 47.
[10] M. Fuss, H.-U. Siehl, B. Olenyuk, P. J. Stang, *Organometallics* **1999**, *18*, 758−769.
[11] Z. Qin, M. C. Jennings, R. J. Puddephatt, *Chem. Commun.* **2001**, 2676−2677.
[12] H.-Q. Liu, S.-M. Peng, C. M. Che, *Chem. Commun.* **1995**, 509−510.
[13] G. Bruno, to be published.
[14] D. J. Craik, G. C. Levy, *Top. Carbon-13 NMR Spectrosc.* **1984**, *4*, 239.
[15] R. Diamond, *Acta Crystallogr., Sect. A* **1969**, *25*, 43−55.
[16] Bruker, *XSCANS*, release 2.31, Bruker AXS Inc., Madison, Wisconsin, **1999**.
[17] G. M. Sheldrick, *SHELXTL*, VMS version 5.05, Siemens Analytical X-ray Instruments Inc., Madison, Wisconsin, **1991**.
[18] A. Altomare, O. Cascarano, C. Giacovazzo, A. Guagliardi, M. C. Burla, G. Polidori, M. Camalli, *J. Appl. Crystallogr.* **1994**, *27*, 435−436.
[19] G. M. Sheldrick, *SHELXL-97, Program for Crystal Structure Refinement*, Univ. of Göttingen, Germany, **1997**.
[20] M. Nardelli, *J. Appl. Crystallogr.* **1985**, *28*, 659; release November **1999**.
[21] G. M. Sheldrick, *Acta Crystallogr., Sect. A* **1990**, *46*, 467.
Received January 16, 2003

  